Investigational New Drugs (2019) 37:1187–1197
https://doi.org/10.1007/s10637-019-00751-1

PRECLINICAL STUDIES

Novel palladium (II) complexes with tetradentate thiosemicarbazones. Synthesis, characterization, in vitro cytotoxicity and xanthine oxidase inhibition

Dilşad Özerkan[1] · Onur Ertik[2] · Buşra Kaya[2] · Serap Erdem Kuruca[3] · Refiye Yanardag[2] · Bahri Ülküseven[2]

Received: 10 January 2019 / Accepted: 25 February 2019 / Published online: 14 March 2019

Summary
In vitro cytotoxicity and xanthine oxidase inhibition capabilities were investigated for five palladium (II) chelate complexes. The palladium complexes were synthesized by starting from S-alkyl-thiosemicarbazones where the alkyl component is methyl, ethyl, propyl or butyl. The solid complexes are characterized by elemental analysis and spectroscopic techniques (UV-visible, IR and 1H NMR). In order to be able to verify the N2O2-type thiosemicarbazidato ligand (L2−) structure in the square planar geometry, complex 1 has been studied as a representative by using single crystal X-ray crystallography. The in vitro cytotoxic activity measurements were carried out in HepG2 and Hep3B hepatocellular carcinomas, HCT116 colorectal carcinoma, and 3 T3 mouse fibroblast cell lines. The palladium complexes exhibited notable cytotoxic activities in all cell lines at lower μM concentrations compared to the standard chemicals, cisplatin and allopurinol. IC_{50} values were determined between 0.42 ± 0.01 and 12.01 ± 0.37 μg/ml in examining the antixanthine oxidase abilities of the complexes. Two complexes with S-methyl group exhibited a high inhibition activity on the xanthine oxidase. The results indicated that these complexes could be used as active pharmaceutical ingredients.

Keywords Palladium · Thiosemicarbazone · X-ray analysis · Cytotoxicity · Xanthine oxidase

Introduction

Synthesis and characterization of palladium complexes are subject of current interest due to their biological activities beside their interesting structural features such as catalytic [1–3] and optical sensing [4]. Complexes of ON, ONS, and ONN-chelating Schiff bases and especially thiosemicarbazone ligands have been extensively used in examining the biological properties of palladium compounds. Prominent biological properties of compounds of these classes are antimicrobial [5, 6], antitumor [7, 8], and antiviral [9] activities, beside cytotoxicity on detrimental cells of mammalian [10–12] and abilities of DNA binding [13, 14].

In last decade, enzyme inhibition has been added among these investigated properties of palladium complexes with bi- and tri-dentate ligands [15–18]. Possible correlation between enzyme activity and diseases is an important reason for increasing interest in inhibition researches. For example, some studies have shown that the effect of the Triapine (3-aminopyridine-2-carboxaldehyde-thiosemicarbazone) is mediated by the inhibition of ribonuclease reductase enzyme and by the disruption of DNA synthesis [19, 20]. The relationship between enzyme inhibition and other therapeutic effects are not always meaningful, but in order to reveal potential biological effects of a new molecule, the biological activities such as antitumor and antiviral are frequently published with interaction results between test molecules and enzymes.

Xanthine oxidase (XO) is an enzyme with versatile functions. The elevated levels of xanthine oxidoreductase (XOR) (XOR = xanthine dehydrogenase + xanthine oxidase) were observed in the plasma of patients with different types of

✉ Serap Erdem Kuruca
sekuruca@istanbul.edu.tr

[1] Department of Genetic and Bioengineering, Faculty of Engineering and Architecture, Kastamonu University, Kastamonu, Turkey

[2] Department of Chemistry, Engineering Faculty, Istanbul University-Cerrahpasa, 34320, Avcilar, Istanbul, Turkey

[3] Deparment of Physiology, Istanbul Medical Faculty, Istanbul University, Fatih/Çapa, 34093, Istanbul, Turkey

cancer [21]. An increased XO activity was also reported in human laryngeal well- differentiated squamous cell carcinomas [22]. Similarly, XOR level was found to be relatively high in some breast cancer cell lines, and therefore a potential role of XO was suggested for suppressing breast cancer pathogenesis [23]. Furthermore, XO can form oxidative agents such as hydrogen peroxide (H2O2) and superoxide (O2 •−) by reducing oxygen molecule (O2). It is vitally important to check the XO level to prevent possible damages arising from these reactive chemical species. In this regard, it is expected to find a XO- inhibitor for designated treatment, for example for cancer diseases, instead of chemicals with many side effects like allopurinol [24, 25].

In recent years several uniformity observed between platinum (II) and palladium (II) complexes were thought to be an anti-cancer agent candidate [26, 27]. However, palladium (II) complexes are 105-fold faster than platinum (II) complexes and have better solubility. Therefore, in recent years investigators have focused on synthesizing new palladium complexes for treatment of several cancer types.

As mentioned above, many palladium complexes have been investigated in a number of studies in the context of cytotoxicity against non-normal mammalian cells and for some additional biological effects. However, palladium complexes with N2O2-type Schiff ligand based on thiosemicarbazide have not been investigated yet with enzyme inhibition and cytotoxicity properties together. We present synthesis and characterization of five palladium (II) chelate complexes with tetra dentate thiosemicarbazidato ligands (Fig. 1). To explicate the usefulness of the complexes as medicine, their xanthine oxidase (XO) inhibition capabilities were determined, and these complexes were applied on HepG2 and Hep3B human hepatocarcinoma cells, HCT116 human colon cancer. Mouse fibroblast cells (3 T3) were used to recognize the effect of these test samples on healthy cells.

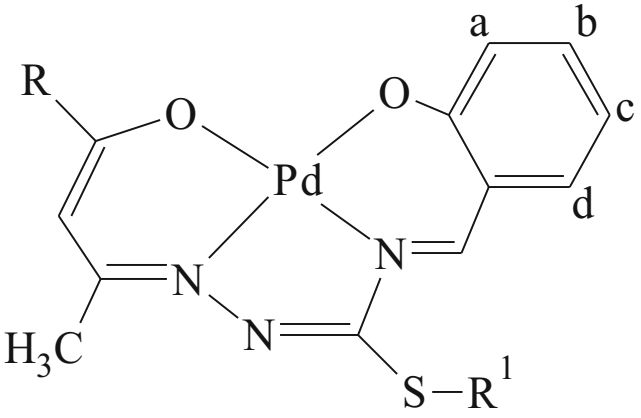

Fig. 1 The palladium (II) complexes. **R**, **R**^{1}: CH_3, CH_3 (**1**); CH_3, C_2H_5 (**2**); CH_3, C_3H_7 (**3**); CH_3, C_4H_9 (**4**); C_6H_5, CH_3 (**5**)

Material and methods

Apparatus, method

Analytical data were obtained with a Thermo Finnigan Flash EA 1112 analyzer. Infrared spectra of the compounds were measured using an ATR unit in 4000–600 cm^{-1} range by using an Agilent Carry 630 FTIR-ATR spectrophotometer. UV-visible spectra were obtained an UV-2600 (Shimadzu) UV/visible spectrophotometer. 1H- NMR was recorded Varian UNITY INOVA 500 MHz NMR spectrometer.

For X-ray analysis, a dark orange-cube-like crystal, approximate dimensions 0.200 mm × 0.200 mm × 0.200 mm, was used for the X-ray crystallographic analysis. The X-ray intensity data were measured on a Bruker D8 VENTURE system equipped with a multilayer monochromator and a Mo Kα Sealed Tube (λ = 0.71073 Å). Data were corrected for absorption effects using the multi-scan method (SADABS) [28]. The ratio of minimum to maximum apparent transmission was 0.797. The structure was solved and refined using the Bruker SHELXTL Software Package [29, 30].

Synthesis of starting materials

The S-alkyl-thiosemicarbazones were prepared according to literature [31]. Melting point (°C), yields (%), elemental analysis, IR (cm^{-1}), UV-Vis (CDCl3) and 1H-NMR (500 MHz, ppm) data of the thiosemicarbazones are given below by indicating S-alkyl group and acetyl acetone (acac) moiety.

S-methyl, acac: 169. 70. Anal. Calc. for $C_7H_{13}N_3OS$ (187.26 g/mol): C, 44.90; H, 7.00; N, 22.44; S, 17.12. Found: C, 44.76; H, 6.88; N, 22.19; S, 16.70%. UV-Vis: 240 (4.4), 255 (4.4), 358 (3.8). IR: $\nu_{as}(NH_2)$ 3327, $\nu_s(NH_2)$ 3341, ν(OH) 3260, δ(NH_2), ν(C=N^1), ν(N^2 = C) 1637–1539, ν(C-S) 738. ^{1}H NMR: 9.39, 8.95 (*cis*/*trans* ratio:1/3, s, 2H, N*H*$_2$), 7.70 (s, 1H, O*H*), 3.73 (s, 1H, C*H*-), 2.59 (s, 3H, S-C*H*$_3$), 2.08 (s, 3H, C-C*H*$_3$), 1.73 (s, 3H, C-C*H*$_3$).

S-ethyl, acac: 145. 55. Anal. Calc. for $C_8H_{15}N_3OS$ (201,28 g/mol): C, 47.74; H, 7.51; N, 20.88; S, 15.93. Found: C, 47.61; H, 7.34; N 20.55; S 15.69%. UV-vis: 215 (4.58), 256 (5.04), 351 (3.6). IR: $\nu_{as}(NH_2)$ 3171, $\nu_s(NH_2)$ 3093, ν(OH) 3242, δ(NH_2), ν(C=N^1), ν(N^2 = C): 1638–1557, ν(C-S) 782. ^{1}H NMR: 9.39, 8.83 (*cis*/*trans* ratio:2/1, s, 2H, N*H*$_2$), 7.78, 7.54 (*cis*/*trans* ratio:1, s, 1H, O*H*), 3.28 (m, 2H, S-C*H*$_2$-), 3.17 (s, 1H, C*H*-), 2.08 (s, 3H, C-C*H*$_3$), 1.76 (s, 3H, C-C*H*$_3$), 1.29 (t, 3H, -C-C*H*$_3$).

S-propyl, acac: 139. 60. Anal. Calc. for $C_9H_{17}N_3OS$ (215,31 g/mol): C, 50.20; H, 7.96; N, 19.52; S, 14.89. Found: C, 49.94; H, 7.74; N 19.37; S, 14.65%. UV-vis: 216 (4.45), 256 (4.89), 298 (2.6). IR: $\nu_{as}(NH_2)$ 3153,

$\nu_s(NH_2)$ 3101, ν(OH) 3246, δ(NH_2), ν(C=N^1), ν(N^2 = C): 1638–1550, ν(C-S) 767. ^{1}H NMR: 9.39, 8.83 (*cis*/*trans* ratio:2/1, s, 2H, N*H*$_2$), 7.78, 7.54 (*cis*/*trans* ratio:1, s, 1H, O*H*), 3.28 (m, 2H, S-C*H*$_2$-), 3.12 (s, 1H, C*H*-), 2.07 (s, 3H, C-C*H*$_3$), 1.7 (s, 3H, C-C*H*$_3$), 1.61 (m, 3H, -C-C*H*$_3$), 0.97 (m, 2H, C-C*H*$_2$).

S-butyl, acac: 130. 45. Anal. Calc. for $C_{10}H_{19}N_3OS$ (229,34 g/mol): C, 52.37; H, 8.35; N, 18.32; S, 13.98. Found: C, 51.88; H, 8.18; N, 18.18; S 13.69%. UV-vis: 215 (4.57), 256 (5.07), 303 (2.47). IR: $\nu_{as}(NH_2)$ 3178, $\nu_s(NH_2)$ 3083, ν(OH) 3240, δ(NH_2), ν(C=N^1), ν(N^2 = C): 1638–1558, ν(C-S) 733. ^{1}H NMR: 9.39, 8.82 (*cis*/*trans* ratio:2/1, s, 2H, N*H*$_2$), 7.77, 7.54 (*cis*/*trans* ratio:1, s, 1H, O*H*), 3.27 (m, 2H, S-C*H*$_2$-), 3.08 (s, 1H, C*H*-), 2.1 (s, 3H, C-C*H*$_3$), 1.77 (s, 3H, C-C*H*$_3$), 1.59 (m, 2H, C-C*H*$_2$), 1.4 (m, 2H, C-C*H*$_2$), 0.9 (m, 3H, C-C*H*$_3$).

S-methyl, benzoyl-acac: 94. 60. Anal. Calc. for $C_{12}H_{15}N_3OS$ (249,33 g/mol): C, 57.81; H, 6.06; N, 16.85; S, 12.85. Found: C, 57.75; H, 6.00; N, 16.74; S, 12.67. UV-vis: 247 (4.89), 321 (4.52), 386 (5.03). IR: $\nu_{as}(NH_2)$ 3301, $\nu_s(NH_2)$ 3196, ν(OH) 3421, δ(NH_2), ν(C=N^1), ν(N^2 = C) 1685–1543. ^{1}H NMR: 7.96–6.65 (m, 5H, aromatic), 6.60, 6.51 (*cis*/*trans* ratio:1/3, s, 2H, N*H*$_2$), 6.45 (s, 1H, O*H*), 5.8 (s, 1H, C*H*-), 2.44 (s, 3H, S-C*H*$_3$), 2.29 (s, 3H, C-C*H*$_3$).

Synthesis of palladium(II) complexes

The palladium(II) complexes (1–5) were prepared by mixing the starting materials in ethanol with a freshly prepared Li2[PdCl4] in equimolar amounts (1 mmol). The reaction mixture was stirred for 2 h at 50 °C. After addition of triethylamine (0.1 mmol) precipitated solids were filtered off, washed with ethanol and dried.

The m.p. (°C), yields (%), elemental analysis, characteristic UV–vis [λmax (log ε), nm (dm^3 cm^{-1} M^{-1})], and characteristic IR (cm^{-1}) bands, and 1H NMR (CDCl3, ppm) data of 1–5 are given below.

1: 230. 25. *Anal. Calc*. for $C_{14}H_{15}N_3O_2SPd$ (395,77 g/mol): C, 42.49; H, 3.82; N, 10.62; S, 8.10. Found: C, 42.25; H, 3.78; N, 10.48; S, 7.92%. UV-Vis: 240 (5.14), 328 (5.09), 474 (4.9), 519 (4.6). IR: ν(C=N^1) 1606, ν(N^2 = C) 1572, ν(N^4 = C) 1560, ν(C-O) 1141,1116, ν(C-S) 755. ^{1}H NMR: 8.16 (s, 1H, N=C*H*), 7.50 (m, 2H, *c,d*), 7.35 (d, *J* = 8.79,1H, *a*), 6.76 (t, *J* = 6.35, *J* = 15.62, 1H, *b*), 5.24 (s, 1H, =C*H*), 2.78 (s, 3H, S-C*H*$_3$), 2.42 (s, 3H, C-C*H*$_3$), 2.26 (s, 3H, C-C*H*$_3$).

2: 216. 25. *Anal. Calc*. for $C_{15}H_{17}N_3O_2SPd$ (409.8 g/mol): C, 43.96; H, 4.18; N, 10.25; S, 7.82. Found: C, 43.87; H, 4.04; N, 10.02; S, 7.56%. UV-Vis: 240 (5.01), 328 (4.95), 474 (4.74), 522 (4.46). IR: ν(C=N^1) 1607, ν(N^2 = C) 1574, ν(N^4 = C) 1558, ν(C-O) 1137,1114, ν(C-S) 762. ^{1}H NMR: 8.23 (s, 1H, N=C*H*), 7.51 (m, 2H, *c,d*), 7.38 (d, *J* = 8.78,1H, *a*), 6.75 (t, *J* = 6.34, *J* = 15.61, 1H, *b*), 5.26 (s, 1H, =C*H*), 3.29 (m, 2H, S-C*H*$_2$), 2.43 (s, 3H, C-C*H*$_3$), 2.3 (s, 3H, C-C*H*$_3$), 1.46 (t, *J* = 15, 3H, C-C*H*$_3$).

3: 170. 22. *Anal. Calc*. for $C_{16}H_{19}N_3O_2SPd$ (423.82 g/mol): C, 45.34; H, 4.52; N, 9.91; S, 7.57. Found: C, 45.23; H, 4.37; N, 9.78; S, 7.46%. UV-Vis: 240 (5.07), 328 (5.01), 475 (4.8), 522 (4.46). IR: ν(C=N^1) 1606, ν(N^2 = C) 1576, ν(N^4 = C) 1561, ν(C-O) 1140,1115, ν(C-S) 759. ^{1}H NMR: 8.23 (s, 1H, N=C*H*), 7.50 (m, 2H, *c,d*), 7.36 (d, *J* = 9.27,1H, *a*), 6.74 (t, *J* = 6.34, *J* = 15.61, 1H, *b*), 5.24 (s, 1H, =C*H*), 3.26 (t, *J* = 6.84, *J* = 14.16, 2H, S-C*H*$_2$), 2.41 (s, 3H, C-C*H*$_3$), 2.3 (s, 3H, C-C*H*$_3$), 1.85 (m, 2H, C-C*H*$_2$), 1.09 (t, *J* = 7.32, *J* = 18.06, 3H, C-C*H*$_3$).

4: 151. 20. *Anal. Calc*. for $C_{17}H_{21}N_3O_2SPd$ (437.85 g/mol): C, 46.63; H, 4.83; N, 9.60; S, 7.32. Found: C, 46.55; H, 4.65; N, 9.48; S, 7.16%. UV-Vis: 240 (5.08), 329 (5.03), 474 (4.83), 520 (4.52). IR: ν(C=N^1) 1607, ν(N^2 = C) 1575, ν(N^4 = C) 1558, ν(C-O) 1142,1117, ν(C-S) 760.^{1}H NMR: 8.23 (s, 1H, N=C*H*), 7.50 (m, 2H, *c,d*), 7.35 (d, *J* = 9.27,1H, *a*), 6.75 (t, *J* = 6.34, *J* = 15.62, 1H, *b*), 5.22 (s, 1H, =C*H*), 3.27 (t, *J* = 6.84, *J* = 14.16, 2H, S-C*H*$_2$), 2.41 (s, 3H, C-C*H*$_3$), 2.27 (s, 3H, C-C*H*$_3$), 1.83 (m, 2H, C-C*H*$_2$), 1.12 (m, 5H, C*H*$_2$-C*H*$_3$).

5: 180. 28. *Anal. Calc*. for $C_{19}H_{17}N_3O_2SPd$ (457.84 g/mol): C, 49.84; H, 3.74; N, 9.18; S, 7.00. Found: C, 49.75; H, 3.59; N, 9.01; S, 6.71%. UV-Vis: 241 (5.21), 292 (5.02), 331 (4.94), 490 (4.45), 528 (4.24). IR: ν(C=N^1) 1607, ν(N^2 = C) 1579, ν(N^4 = C) 1566, ν(C-O) 1139,1120, ν(C-S) 744. ^{1}H NMR: 8.1 (s, 1H, N=C*H*), 7.91 (m, 2H, *e,j*), 7.4 (m, 2H, *c,d*), 7.32 (m, 3H, *f,g,h*),7.27 (d, *J* = 8.79,1H, *a*), 6.76 (t, *J* = 8.3, *J* = 16.11, 1H, *b*), 5.82 (s, 1H, =C*H*), 2.73 (s, 3H, S-C*H*$_3$), 2.46 (s, 3H, C-C*H*$_3$).

Cytotoxicity assay

The MTT is a colorimetric assay based on the ability of living cells the reducing 3-[4,5-dimethylthiazol-2-yl]-2,5 diphenyl tetrazolium bromide to formazan. The Mossman's method, that is a version of MTT, modified by our laboratory, was used to determine the cytotoxic effects [32]. Stock solutions of these compounds were set at 5 mg/ml in (Dimethyl sulfoxide) DMSO. Each of the compounds were arranged in different concentrations (10 μg/ml, 7 μg/ml, 5 μg/ml and 3.5 μg/ml) for assessment of inhibitory concentration 50 (IC_{50} = the concentration of the compound that inhibited 50% cells) value.

After then, 10 μl was added to 96 well plates each one as triplicate.

HepG2, Hep3B, HCT116 and 3 T3 cells were plated in 96 multi-well culture plates as 10^4cells/well and incubated at 37 °C in 5% CO2 atmosphere for 72 h, respectively. 3 T3 cells were used as healthy control cells. Cisplatin and allopurinol (chemotherapy drugs) were used as negative control. MTT was added to wells as 10 μl after the incubation time and incubation continued for 3 h at 37 °C. At the end of the incubation, cells were lysed by addition of 100 μl of DMSO. The optical density (OD) of formazan was measured with 560 nm test wavelength and a 620 nm reference wavelength by ELISA multi-well spectrophotometer (Diagnostics Pasteur LP 400). The absorbance of negative control was subtracted from all Palladium added group results. Cytotoxicity index (CI) was calculated with the following formula compared to control:

$$\%\text{CI (Cytotoxicity index)} = 1-\text{OD treated wells}/\text{OD control wells} \times 100.$$

Also, IC_{50} was calculated from dose- response curves. These experiments were repeated at least 3 times independently.

Xanthine oxidase inhibitory activity

XO inhibitory activity was determined spectrophotometrically via using xanthine as the substrate [33]. The assay mixture, consisted of samples, phosphate buffer (pH:7.5) and xanthine oxidase enzyme solution (0,1 U/mL in phosphate buffer, pH:7.5) which were prepared immediately before use. After preincubation at 25 °C for 15 min, the reaction was initiated by substrate solution. The assay mixture was incubated for 30 min. Then, the reaction was stopped by HCl. Absorbance value was measured at 290 nm using UV spectrophotometer. XO inhibitory activity was expressed as the percentage of inhibition of XO in the above assay system calculated as:

$$\text{Inhibition}\ (\%) = (1-[B/A]) \times 100$$

Where A represents the activity of the enzyme without sample and B the activity of XO in the presence of the sample. Allopurinol was used as the positive control. For XO enzyme inhibition, the results are given as half maximal inhibitory concentration (IC_{50}) values, calculated from the regression equations prepared from the concentrations of samples. Inhibition types for the palladium complexes were calculated by Lineweaver Burk curves for XO enzyme [34].

Results

Synthesis and structural characterization

The S-alkyl thiosemicarbazones were condensed with salicylaldehyde by template effect of the palladium(II) ion. The complexes, 1–5, in the expected compositions were comprised of the reactions in ethanol (Fig. 1). The complexes are soluble in alcohol and chlorinated hydrocarbons.

The electronic absorption bands of the thiosemicarbazones were recorded in 10^{-5} M chloroform solution. In the spectra, the expected $\pi \rightarrow \pi^*$ and $n \rightarrow \pi^*$ bands of the thiosemicarbazone molecules are at 240, 292 and in the range of 328–331 nm. The electronic spectra of the complexes, 1–5, at 10^{-6} M concentration included a quite broad band having the peak at 474–490 nm and a shoulder at 519–528 nm in addition to the band originating from the reactant thiosemicarbazone. The spectra do not clearly show the common bands of a square plane geometry. However, the peak and shoulder values are in the wavelengths which can be attributed to the $1A1g \rightarrow 1A2g$ and $1A1g \rightarrow 1Eg$ transitions of D4h symmetry.

The S-alkyl thiosemicarbazones can be defined by observing the infrared spectrum bands attributable to imine and thioamide groups, νas(NH2), νs(NH2), δ(NH2), ν(C=N1), and ν(N2 = C). In the region of 1685–1539 cm^{-1}, the bands arising from the imine and thioamide groups were fundamentally altered after complex formation, and vibrations of OH and NH2 groups between 3421 and 3093 cm − 1disappered because of deprotonation of phenolic hydroxyl and condensation of NH2 group on thioamide. The formation of the palladium(II) complexes can also be checked by 1H NMR spectra. Proton signals of phenolic OH and NH2 haven't been observed like in the infrared spectrum.

A singlet signal equivalent to one proton indicated the formation of new imine group (N4 = CH) and therefore completion of the template reaction. 1H NMR spectra of 1–5 showed expected chemical shifts for the phenyl, acetyl and S-alkyl protons.

X-ray crystallographic analysis of complex 1 was performed to prove the dibasic thiosemicarbazidato ligand structure and square planar complex geometry. For X-ray analysis, a dark orange-cube- like crystal, approximate dimensions 0.200 mmx 0.200 mm × 0.200 mm, was chosen and data was collected using the multi-scan method (SADABS) [28]. The ratio of minimum to maximum apparent transmission was 0.797. The structure was solved and refined using the Bruker SHELXTL Software Package [29, 30]. ORTEP diagram of complex 1 is shown in Fig. 2. Refinement data and coordination bond lengths and angles are given in Tables 1 and 2.

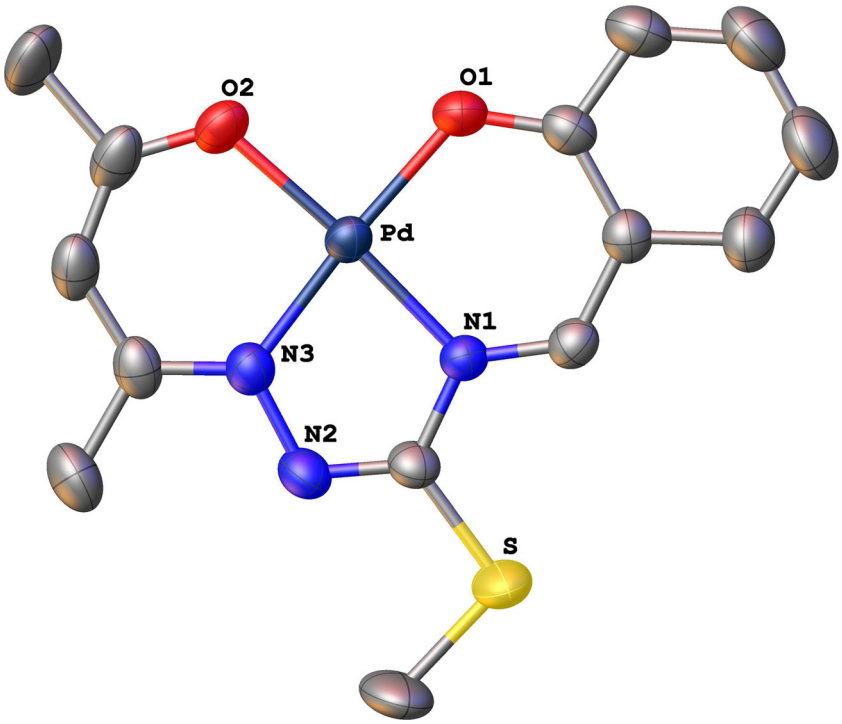

Fig. 2 ORTEP diagram of complex **1** excluding hydrogens

In the complex structure, palladium(II) ion is coordinated by two oxygen atoms and two nitrogen atoms of the thiosemicarbazidato ligand with the donor set consisting of the O1, N1, N2, and O2 atoms. This N2O2 chelating ligand forms by template reaction to form a square plane geometry around the metal center. The chelate complex includes one five-membered and two six-membered chelate rings. The central atom has a distorted square-planar environment according to cis and trans angles of the coordination bonds (Table 2). O1-Pd-N3 and O2-Pd-N1 angles with the values approximately 175° indicate palladium atom slightly above square base. While the bond lengths of the palladium center with O1, PO1, and N1 are in very close values, Pd-N3 bond is longer (ca.0.3 Å).

Cytotoxicity results

The in vitro cytotoxic activity measurements were carried out using HepG2 and Hep3B hepatocellular carcinomas and HCT116 colorectal carcinoma cell lines. The cytotoxic activity of each of test chemicals, complexes 1–5, were found different in every cancer cell line. The IC_{50} values for all cell lines are 3–7 fold lower compared with cisplatin and allopurinol. Besides, the repeated measurements revealed that the test chemicals had a relatively higher cytotoxic effect on Hep3B cells than HepG2 cells (Table 3).

In experiments, cells of HepG2, that are proliferated in colonies, were observed. Especially increase in granulation and round shaped cells, loss of typical cell morphology with the collapse of cell colonies were seen in HepG2 cells treated with complexes 1–5. A remarkable decrease in the number in Hep3B cells, spread out on the surface, was observed after treatment with the palladium (II) complexes,. It was noted that the cells were overgrown and palladium residues are predominant in overgrown cells, which seem like small islets in treatment with high dose of the test chemicals (Fig. 3).

The HCT116 group of cells were spread over the surface. In contrast to the increase in volume and fusiform shape of some of the HCT116 cells in which the palladium(II) complexes were applied, some cells showed shrinkage and rounded shape. It is notable that the numbers of cells and connections between cells have decreased. Mouse fibroblast cells, 3 T3 cells were not only overgrown, also they diffused in more than one layer. So it was not possible to properly focus on one of the surfaces, and clear photos could not be captured. The palladium accumulation in 3 T3 fibroblast cells was very low, and the number of living cells decreased in comparison with the control group (Fig. 4).

After 72 h treatment of palladium(II) complexes, cell viability was determined with MTT. According to the results Hep3B and HCT116 cells were affected more than HepG2 and 3 T3 cells were. Complexes 1, 2 and 4 are determined

Table 1 Summary of crystal and refinement data for 1

	1
Empirical formula	$C_{14}H_{15}N_3O_2PdS$
Crystal colour, habit	dark orange cube
Crystal size (mm)	0.200 × 0.200 × 0.200
Formula weight	395.75
Temperature (K)	304(0) K
Wavelength (Å)	0.71073
Crystal system	monoclinic
Space group	P 1 21/c 1
Cell dimensions (Å, °)	a = 9.246(4)
	b = 12.555(6)
	c = 13.081(6)
	α = 90
	ß = 95.957(16)
	γ = 90
Cell volume ($Å^3$)	1510.3(12)
Cell Formula units (Z)	4
Density (calculated)	1.741
Absorption coefficient(mm^{-1})	1.374
F_{000}	792
h, k, l ranges	−13 < =h < =10
	−17 < =k < =17
	−18 < =l < =18
Reflections collected	17,567
Independent reflections	4036 [R(int) = 0.0315]
Data/restraints/parameters	4036/0/193
Goodness of fit indicator	1.160
Final R indices	3416 data; I > 2σ(I) R1 = 0.0384, wR2 = 0.1073
	All data R1 = 0.0497, wR2 = 0.1228
Largest diff. peak and hole	0 0.759 and − 1.026 $eÅ^{-3}$

more effective on cell survival at Hep3B and HCT116 cells. Cell viability of 3 T3 cells are found to be higher than 70%, partially similar to HepG2 in all experimental groups (Fig. 5).

Enzyme inhibition results

The xanthine oxidase inhibition values of complexes 1–5 are given in Table 4. All samples exhibited an increase anti-xanthine oxidase activity in a dose dependent manner. The inhibition mechanisms of the palladium complexes were uncompetitive.

Table 2 Selected bond lengths (Å) and angles (°) for **1**

Bond	Distance	Bond	Angle
Pd-O1	1.989(3)	O1-Pd-N1	94.55(14)
Pd-O2	1.989(3)	O1-Pd-N3	175.66(15)
Pd-N1	1.989(3)	O2-Pd-O1	89.66(14)
Pd-N3	1.926(4)	O2-Pd-N3	94.58(15)
		O2-Pd-N1	175.79(14)
		N1-Pd-N3	81.21(15)

Table 3 The effect of palladium complexes on different cancer cell lines

Compounds	IC_{50} values in μg/ml			
	HEP3B	HEPG2	HCT116	3T3*
1	4.02	7.46	3.01	7,09
2	3.61	6.73	5.56	6.18
3	4.36	6.29	2.73	5.86
4	3.55	6.34	2.77	5.92
5	3.62	6.98	4.92	6.20
Cisplatin	22.05	18.34	21.25	11.98
Allopurinol	17.44	13.04	8.64	11.33

Proliferation was evaluated by MTT. IC_{50} values were taken after 72 h

*Healthy cell line

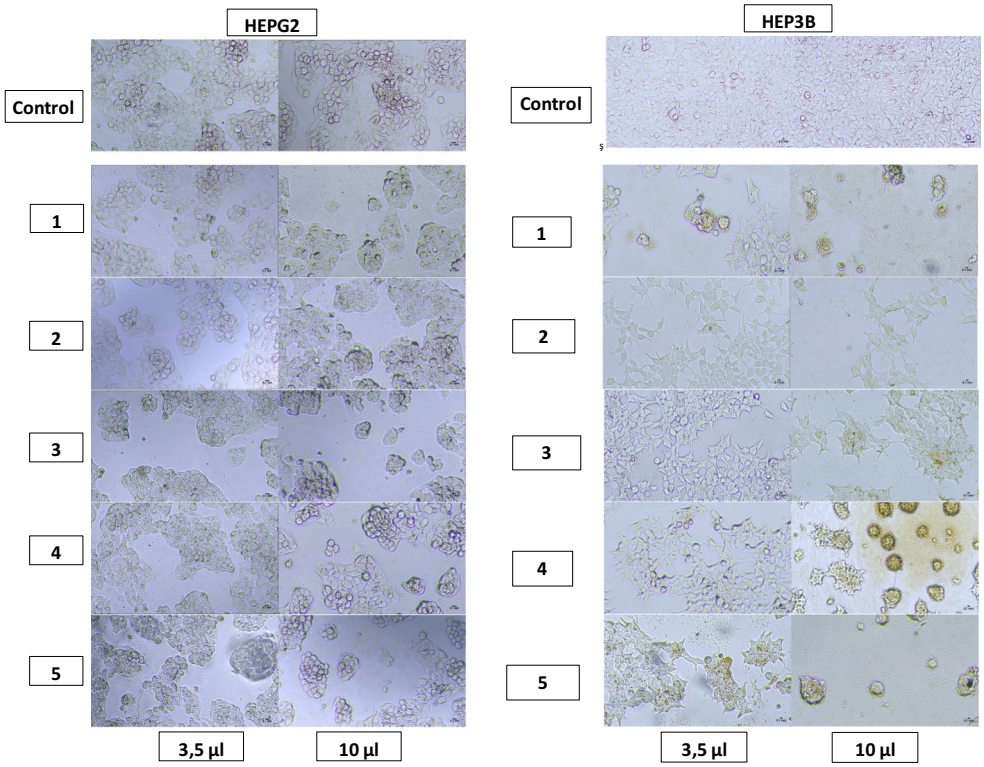

Fig. 3 Treatment of palladium(II) complexes low to high concentrations on HepG2 and Hep3B hepatoblastoma cell lines are seen. Magnification: X100

The highest anti xanthine oxidase activity was found for complexes 1 and 5, which have the IC_{50} values, as 0.42 and 0.66 µg/ml, respectively. Complexes 2 and 3 gave the IC_{50} values, 4.09 and 3.87 µg/ml, representing an average XO inhibition efficiency. Complex 4 has a relatively low inhibition capacity with 12.01 µg/ml compared to the others.

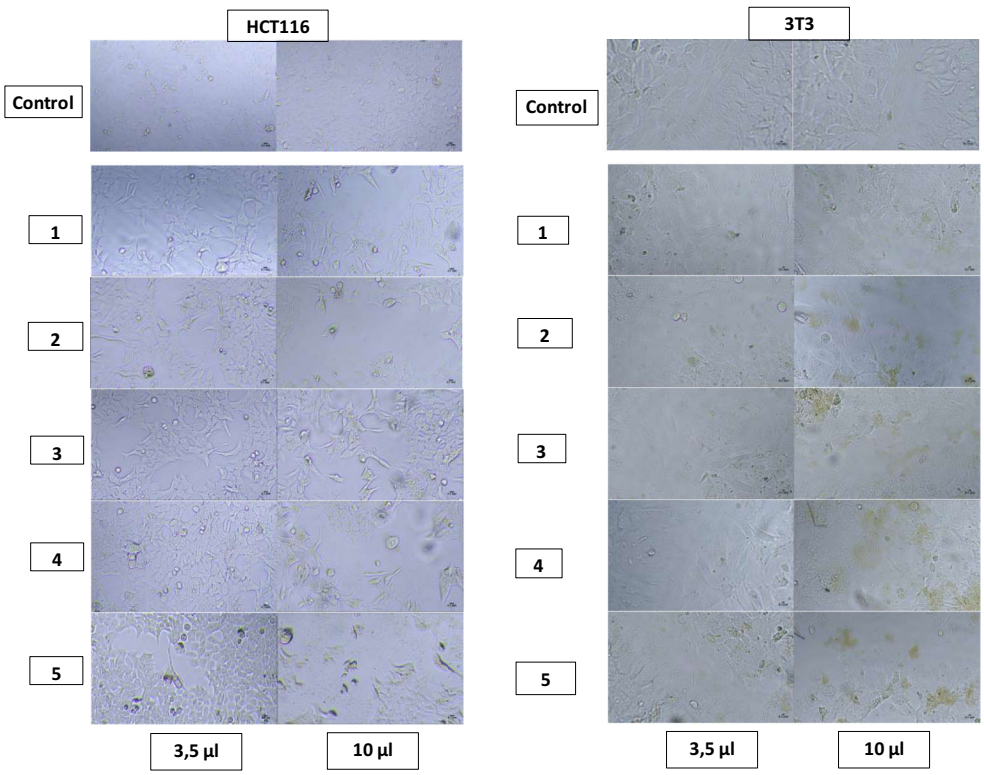

Fig. 4 Demonstration of palladium (II) complexes between HCT116 colon cancer and 3 T3 fibroblast cells according to lower to higher concentrations. Magnification: X100

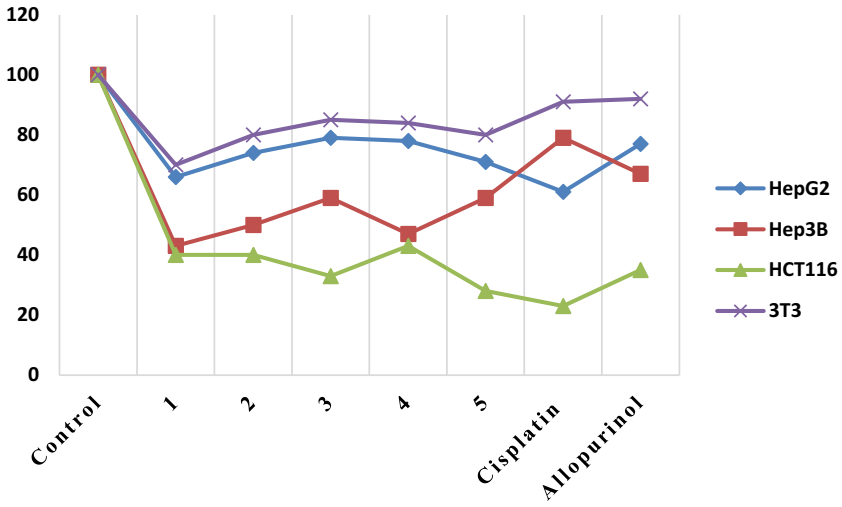

Fig. 5 Cell viability of all colon and liver cancers with fibroblasts were quantified by trypan blue exclusion

Discussion

Recently, the use of inorganic substances with antitumor effects in cancer therapy has been of interest [35]. Thiosemicarbazones among them have an effective therapeutic activity against bacterial and viral infections, tuberculosis, leprosy and cancer. Biological activities have also been observed to vary depending on the aldehyde or ketone group they have [36]. Biological activity in such systems generated by changes in the metal atom itself, by displacement reactions involving more unstable extra planar ligands, or with substituents attached to the ring system [37]. At the same time, research shows that the biological activities of ligands are increased by complexity of metal formation [38]. The cytotoxic effects of thiosemicarbazones like iron, zinc, copper, nickel, palladium, platinum, ruthenium, and other metals were observed on standard tumor cell lines of in various studies The mechanisms behind these are still being investigated and unclear, but there is a therapeutic benefit of this selective effect on normal and cancer cells [39, 40].

From this point of view, five of new palladium (II) complexes with N2O2-type thiosemicarbazidato ligand were synthesized and characterized. The cytotoxicity and xanthine oxidase (XO) inhibition features of the complexes were examined in order to understand their influences on vital continuum and to determine their possible use as medicine.

Our findings showed that palladium (II) complexes apparently caused cell death, as in all other studies. The cytotoxicity tests of complexes 1–5 exhibited lower IC50 values for hepatoma cancer cells compared with cisplatin and allopurinol that are used as chemotherapy drugs. The higher cytotoxicity on Hep3B cells than HepG2 cells are extremely important when considering the differences between the two cell lines. Because, HepG2 is hepatitis B virus negative, wild-type p53 and nontumorigenic, but Hep3B is hepatitis B virus positive, p53 deficient and tumorigenic. [41–43]. The effectiveness of complexes 1–5 at low doses on tumorigenic cells and at relative high doses on non-tumorigenic cells (HepG2) may be indicative of therapeutic significance of these chemicals due to the low possibility of affecting normal cells (3 T3). These selective and protective effects are significant in cancer treatment. Since it is known that palladium compounds are hepatotoxic, the dose differences between the two cell lines are even more noteworthy. Complexes 1–5 were also effective at low doses in tumorigenic HCT116 cells as well, which indicates a potential benefit in the treatment of colorectal cancers.

Beneficial biological effects such as antitumoral and antiviral activities are frequently evaluated by the results of interactions between tested molecules and some enzymes. The relationship between enzyme inhibition and other therapeutic effects is not always meaningful. However, antitumoral and antiviral activities are frequently assessed by the results of interactions between the molecules and enzymes tested to demonstrate the potential biological effect of a new molecule. Reactive oxygen species (ROS) and free radicals that enter the tissues can damage important biological molecules such as DNA, proteins, carbohydrates and lipids. Free radicals can come from outside the body as well as they can be formed as a natural consequence of human metabolism. Endogenous production of free radicals takes place in different ways. Many factors, such as oxygen metabolism in living cells, environmental pollutants, radiation, pesticides, chemotherapy, medical treatment such as radiotherapy, and contaminated water, inevitably lead to the formation of oxygen-derived free radicals. Reactive oxygen species are also produced in the body because of many enzyme activities such as lipoxygenase, cyclooxygenase, xanthine oxidase (XO), myeloperoxidase and cytochrome P-450 [44].

Table 4 The xanthine oxidase inhibitor activity of different concentrations Pd(II) complexes

Chemical Compounds and Standard	Concentration (μg/ml)	Inhibition (%)*	IC_{50} (μg/ml)*
1	1	82.63 ± 0.64	0.42 ± 0.01
	0.5	79.63 ± 0.29	
	0.25	37.22 ± 3.67	
	0.1	23.11 ± 0.84	
	0.01	8.39 ± 0.42	
2	5	58.97 ± 2.27	4.09 ± 0.19
	2.5	34.27 ± 1.34	
	1	16.99 ± 2.47	
	0.5	8.33 ± 1.82	
	0.01	6.15 ± 1.22	
3	5	60.76 ± 1.68	3.87 ± 0.13
	1	27.23 ± 1.10	
	0.5	16.60 ± 0.39	
	0.25	4.67 ± 1.62	
	0.1	1.72 ± 1.70	
4	10	41.09 ± 0.94	12.01 ± 0.37
	5	28.09 ± 2.03	
	1	16.20 ± 0.71	
	0.5	7.87 ± 1.49	
	0.25	3.21 ± 1.12	
5	1	66.34 ± 3.20	0.66 ± 0.04
	0.5	48.46 ± 1.49	
	0.25	28.45 ± 2.69	
	0.1	14.63 ± 2.23	
	0.01	5.62 ± 2.20	
Allopurinol	2.5	79.47 ± 0.66	1.06 ± 0.05
	1.	69.09 ± 1.01	
	0.5	47.09 ± 1.67	
	0.25	20.97 ± 3.05	
	0.1	7.73 ± 1.01	

*Mean ± SD

By study, some significant data related to the role of XO inhibition on cytotoxicity was provided. The XO inhibition of complexes 1–5 is extraordinary enough at very small concentrations while the toxic effect was seen at higher concentrations (similarly allopurinol effect). Allopurinol used as standard is frequently preferred as XO inhibitor, but it shows adverse effects such as fatal liver necrosis, nephropathy, allergic reactions and renal failure [45]. For this reason, it is important to discover new inhibitor agents, which have no adverse effect. The new palladium complexes, especially 1 and 5, having IC50 values lower than the allopurinol standard are powerful candidates as XO enzyme inhibitors. Since the inhibitory activity of the complexes, 1 and 5, are higher than that of allopurinol, we can postulate that the possible side effects of these compounds would be lesser than the known effects of allopurinol due to the efficacy at relative low concentration.

The structure-activity relationship was clearly seen by means of the highest inhibition values of S-methyl derivatives (1 and 5), the decrease of activity in S-ethyl (2) and propyl (3) derivatives and lastly the lower IC_{50} value of complex 4 with a butyl group. The inhibition capacity of this complex series seems to depend on the alkyl chain length on the sulfur atom. As known, the molecules with sulfur atoms exhibit remarkable XO inhibitory activity [46]. For the examined test chemicals, it can be considered that the longer alkyl chains reduce the mentioned function of the sulfur atom.

The new palladium complexes have met expectations with both cytotoxicity and enzyme inhibition performances. As a result, it was clearly seen that these complexes have sufficient activity to be used in drug development investigations.

Acknowledgements Supplementary Material Crystallographic data for the structural analysis have been deposited with the Cambridge Crystallographic Data Centre, CCDC No. CCDC 1411477 for complex 1.

We thankful to Ekin Altepe for proofreading.

Funding This study was funded by The Scientific Research Projects Coordination Unit of Istanbul University, Project Number 54237.

Compliance with ethical standards

Conflict of interest All authors declare no conflicts of interest.

Ethical approval This article does not contain any studies with human participants or animals performed by any of the authors.

References

1. Bankston D, Fang F, Huie E, Xie S (1999) Palladium (II) acetate–Tris (triphenylphosphine) rhodium (I) chloride: a novel catalytic couple for the intramolecular heck reaction. J Organ Chem 64: 3461–3466
2. Soh C, Kamilah S, Shamsuddin M (2012) Tetradentate N2O2 chelated palladium (II) complexes: synthesis, characterization, and catalytic activity towards Mizoroki-Heck reaction of aryl bromides. J Chem 2013:1–8
3. Gogoi A, Dewan A, Borah G, Bora U (2015) A palladium salen complex: an efficient catalyst for the Sonogashira reaction at room temperature. New J Chem 39:3341–3344
4. Yaman P, Subasi E, Temel H, Öter O, Celik E (2014) Synthesis, characterization, catalytic applications and optical sensing properties of palladium complexes containing tetradentate schiff bases. Asian J Chem 26
5. Ali MA, Mirza AH, Butcher RJ, Crouse KA (2006) The preparation, characterization and biological activity of palladium (II) and platinum (II) complexes of tridentate NNS ligands derived from S-methyl-and S-benzyldithiocarbazates and the X-ray crystal structure of the [Pd (mpasme) Cl] complex. Transit Met Chem 31:79–87
6. Khan SA, Yusuf M (2009) Synthesis, spectral studies and in vitro antibacterial activity of steroidal thiosemicarbazone and their palladium (Pd (II)) complexes. Eur J Med Chem 44:2270–2274
7. Padhye S, Afrasiabi Z, Sinn E, Fok J, Mehta K, Rath N (2005) Antitumor metallothiosemicarbazonates: structure and antitumor activity of palladium complex of phenanthrenequinone thiosemicarbazone. Inorg Chem 44:1154–1156
8. Garoufis A, Hadjikakou S, Hadjiliadis N (2009) Palladium coordination compounds as anti-viral, anti-fungal, anti-microbial and anti-tumor agents. Coord Chem Rev 253:1384–1397
9. Genova P, Varadinova T, Matesanz AI, Marinova D, Souza P (2004) Toxic effects of bis (thiosemicarbazone) compounds and its palladium (II) complexes on herpes simplex virus growth. Toxicol Appl Pharmacol 197:107–112
10. Afrasiabi Z, Sinn E, Chen J, Ma Y, Rheingold AL, Zakharov LN, Rath N, Padhye S (2004) Appended 1, 2-naphthoquinones as anticancer agents 1: synthesis, structural, spectral and antitumor activities of ortho-naphthaquinone thiosemicarbazone and its transition metal complexes. Inorg Chim Acta 357:271–278
11. Ferraz KS, Ferandes L, Carrilho D, Pinto MC, de Fátima Leite M, EM S–F, Speziali NL, Mendes IC, Beraldo H (2009) 2-Benzoylpyridine-N (4)-tolyl thiosemicarbazones and their palladium (II) complexes: cytotoxicity against leukemia cells. Bioorg Med Chem 17:7138–7144
12. Caires AC (2007) Recent advances involving palladium (II) complexes for the cancer therapy. Anti-Cancer Curr Med Chem 7:484–491
13. Otero L, Vieites M, Boiani L, Denicola A, Rigol C, Opazo L, Olea-Azar C, Maya JD, Morello A, Krauth-Siegel RL (2006) Novel antitrypanosomal agents based on palladium nitrofurylthiosemicarbazone complexes: DNA and redox metabolism as potential therapeutic targets. J Med Chem 49:3322–3331
14. Kalaivani P, Prabhakaran R, Dallemer F, Poornima P, Vaishnavi E, Ramachandran E, Padma VV, Renganathan R, Natarajan K (2012) DNA, protein binding, cytotoxicity, cellular uptake and antibacterial activities of new palladium (II) complexes of thiosemicarbazone ligands: effects of substitution on biological activity. Metallomics 4:101–113
15. Vieites M, Smircich P, Parajón-Costa B, Rodríguez J, Galaz V, Olea-Azar C, Otero L, Aguirre G, Cerecetto H, González M (2008) Potent in vitro anti-Trypanosoma cruzi activity of pyridine-2-thiol N-oxide metal complexes having an inhibitory effect on parasite-specific fumarate reductase. JBIC J Biol Inorg Chem 13:723–735
16. Tetteh S, Dodoo DK, Appiah-Opong R, Tuffour I (2014) Cytotoxicity, antioxidant and glutathione S-transferase inhibitory activity of palladium (II) chloride complexes bearing nucleobase ligands. Transit Met Chem 39:667–674
17. Alyar S, Adem Ş (2014) Synthesis, characterization, antimicrobial activity and carbonic anhydrase enzyme inhibitor effects of salicilaldehyde-N-methyl p-toluenesulfonylhydrazone and its Palladium (II), Cobalt (II) complexes. Spectrochim Acta A Mol Biomol Spectrosc 131:294–302
18. Barra CV, Rocha FV, Morel L, Gautier A, Garrido SS, Mauro AE, Frem RC, Netto AV (2016) DNA binding, topoisomerase inhibition and cytotoxicity of palladium (II) complexes with 1, 10-phenanthroline and thioureas. Inorg Chim Acta 446:54–60
19. Odenike OM, Larson RA, Gajria D, Dolan ME, Delaney SM, Karrison TG, Ratain MJ, Stock W (2008) Phase I study of the ribonucleotide reductase inhibitor 3-aminopyridine-2-carboxaldehyde-thiosemicarbazone (3-AP) in combination with high dose cytarabine in patients with advanced myeloid leukemia. Investig New Drugs 26:233–239
20. Gojo I, Tidwell ML, Greer J, Takebe N, Seiter K, Pochron MF, Johnson B, Sznol M, Karp JE (2007) Phase I and pharmacokinetic study of Triapine®, a potent ribonucleotide reductase inhibitor, in adults with advanced hematologic malignancies. Leuk Res 31: 1165–1173
21. Battelli MG, Polito L, Bortolotti M, Bolognesi A (2016) Xanthine oxidoreductase in cancer: more than a differentiation marker. Cancer Med 5:546–557
22. Kalcio MT, Lu M, Kizilay A, Yilmaz HR, Efkan U, Güleç M, Özturan O, Akyol Ö (2004) Adenosine deaminase, xanthine oxidase, superoxide dismutase, glutathione peroxidase activities and malondialdehyde levels in the serum of patients with head and neck carcinoma. Kulak Burun Bogaz Ihtisas Dergisi 12:16–22
23. Fini MA, Orchard-Webb D, Kosmider B, Amon JD, Kelland R, Shibao G, Wright RM (2008) Migratory activity of human breast cancer cells is modulated by differential expression of xanthine oxidoreductase. J Cell Biochem 105:1008–1026
24. Sathisha KR, Gopal S, Rangappa KS (2016) Antihyperuricemic effects of thiadiazolopyrimidin-5-one analogues in oxonate treated rats. Eur J Pharmacol 776:99–105
25. Onul N, Ertik O, Mermer N, Yanardag R (2018) Synthesis and antioxidant, antixanthine oxidase, and antielastase activities of novel N, S-substituted polyhalogenated nitrobutadiene derivatives. J Biochem Mol Toxicol 32:e22021
26. Coskun MD, Ari F, Oral AY, Sarimahmut M, Kutlu HM, Yilmaz VT, Ulukaya E (2013) Promising anti-growth effects of palladium (II) saccharinate complex of terpyridine by inducing apoptosis on transformed fibroblasts in vitro. Bioorg Med Chem 21:4698–4705
27. Kapdi AR, Fairlamb IJ (2014) Anti-cancer palladium complexes: a focus on PdX 2 L 2, palladacycles and related complexes. Chem Soc Rev 43:4751–4777
28. Sheldrick G (2012) SADABS-2012/1:Bruker/Siemens area detector absorption correction program. Bruker AXS Inc, Madison
29. Sheldrick GM (2008) A short history of SHELX. Acta Crystallogr A: Found Crystallogr 64:112–122

30. Sheldrick GM (2015) SHELXT–Integrated space-group and crystal-structure determination. Acta Crystallogr. C 71:3–8
31. Yamazaki C (1975) The structure of isothiosemicarbazones. Can J Chem 53:610–615
32. Mosmann T (1983) Rapid colorimetric assay for cellular growth and survival: application to proliferation and cytotoxicity assays. J Immunol Methods 65:55–63
33. Abdullahi A, Hamzah RU, Jigam AA, Yahya A, Kabiru AY, Muhammad H, Sakpe S, Adefolalu FS, Isah MC, Kolo MZ (2012) Inhibitory activity of xanthine oxidase by fractions Crateva adansonii. J Acute Dis 1:126–129
34. Lineweaver H, Burk D (1934) The determination of enzyme dissociation constants. J Am Chem Soc 56:658–666
35. Quenelle DC, Keith KA, Kern ER (2006) In vitro and in vivo evaluation of isatin-β-thiosemicarbazone and marboran against vaccinia and cowpox virus infections. Antivir Res 71:24–30
36. Cukurovali A, Yilmaz I, Gur S, Kazaz C (2006) Synthesis, antibacterial and antifungal activity of some new thiazolylhydrazone derivatives containing 3-substituted cyclobutane ring. Eur J Med Chem 41:201–207
37. Altun A, Kumru M, Dimoglo A (2001) Study of electronic and structural features of thiosemicarbazone and thiosemicarbazide derivatives demonstrating anti-HSV-1 activity. J Mol Struct THEOCHEM 535:235–246
38. Saryan LA, Ankel E, Krishnamurti C, Petering DH, Elford H (1979) Comparative cytotoxic and biochemical effects of ligands and metal complexes of .Alpha.-N-heterocyclic carboxaldehyde thiosemicarbazones. J Med Chem 22:1218–1221
39. Rodríguez-Argüelles MC, López-Silva EC, Js Sanmartín, Bacchi A, Pelizzi C, Zani F (2004) Cobalt and nickel complexes of versatile imidazole- and pyrrole-2-carbaldehyde thiosemicarbazones. Synthesis, characterisation and antimicrobial activity. Inorg Chim Acta 357:2543–2552
40. Rodríguez-Argüelles MC, López-Silva EC, Sanmartín J, Pelagatti P, Zani F (2005) Copper complexes of imidazole-2-, pyrrole-2- and indol-3-carbaldehyde thiosemicarbazones: inhibitory activity against fungi and bacteria. J Inorg Biochem 99:2231–2239
41. Knowles BB, Howe CC, Aden DP (1980) Human hepatocellular carcinoma cell lines secrete the major plasma proteins and hepatitis B surface antigen. Science (New York, NY) 209:497–499
42. Knasmuller S, Parzefall W, Sanyal R, Ecker S, Schwab C, Uhl M, Mersch-Sundermann V, Williamson G, Hietsch G, Langer T, Darroudi F, Natarajan AT (1998) Use of metabolically competent human hepatoma cells for the detection of mutagens and antimutagens. Mutat Res 402:185–202
43. Qiu GH, Xie X, Xu F, Shi X, Wang Y, Deng L (2015) Distinctive pharmacological differences between liver cancer cell lines HepG2 and Hep3B. Cytotechnology 67:1–12
44. Mohsen M (2001) Antioxidants and cognitive function. Nutr Rev 59:S75–S82
45. Wang Y, Zhu JX, Kong LD, Yang C, Cheng CH, Zhang X (2004) Administration of procyanidins from grape seeds reduces serum uric acid levels and decreases hepatic xanthine dehydrogenase/oxidase activities in oxonate-treated mice. Basic Clin Pharmacol Toxicol 94:232–237
46. Song JU, Jang JW, Kim TH, Park H, Park WS, Jung S-H, Kim GT (2016) Structure-based design and biological evaluation of novel 2-(indol-2-yl) thiazole derivatives as xanthine oxidase inhibitors. Bioorg Med Chem Lett 26:950–954